Article type: Original manuscript

Abedin Gagani, Norwegian University of Science and Technology (NTNU), Department of Mechanical and Industrial Engineering, Richard Birkelandsvei 2B, 7010 Trondheim. Norway
Email: abedin.gagani@ntnu.no

Micromechanical modeling of anisotropic water diffusion in glass fiber epoxy reinforced composites

Abedin Gagani (a), Yiming Fan (b), Anastasia H. Muliana (b), Andreas T. Echtermeyer (a)

(a) Department of Mechanical and Industrial Engineering, Norwegian University of Science and Technology (NTNU), Norway

(b) Department of Mechanical Engineering, Texas A&M, USA

Abstract

Fluid diffusion in fiber reinforced composites is typically anisotropic. Diffusivity in the fiber direction is faster than in the transverse direction. The reason for this behavior is not yet fully understood. In this work, dealing with glass fiber epoxy composite immersed in distilled water, an experimental procedure for determination of anisotropic diffusion constants from a laminate is presented. The method has the advantage that it does not require sealing of the samples edges because 3-D anisotropic diffusion theory is implemented for obtaining the diffusion constants. A microscale model is presented, where matrix and fiber bundles are modeled separately. The matrix properties have been obtained experimentally and the fiber bundle properties have been deduced by the composite homogenized diffusivity model. The analysis indicates that the anisotropic diffusion of the composite is due to inherent anisotropic properties of the fiber bundles.

Keywords

Fluid diffusion composites; Micromechanical diffusion modelling composites, FE diffusion composites.

List of symbols

$\mathbf{B}^{(\alpha)}$	Subcell concentration matrix
C	Fluid concentration
D	Effective composite diffusivity
$\mathbf{D}^{(f)}$	Fiber diffusivity
$\mathbf{D}^{(m)}$	Matrix diffusivity
$\mathbf{D}^{(\alpha)}$	Subcell diffusivity
$D_{\parallel}$	Parallel diffusivity
$D_{\perp}$	Transverse diffusivity
D_M	Matrix diffusivity
f	Flux through the homogenized composite
$\mathbf{f}^{(\alpha)}$	Flux through the subcell
$f^{(\alpha)}_i$	Flux in direction i through the subcell α
f_i	Homogenized flux through the composite in direction i
h	Thickness
$\mathbf{I_3}$	Identity matrix
l	Length
M	Moisture content
M_∞	Composite moisture equilibrium content
M^M_∞	Matrix moisture equilibrium content
M^V_∞	Void moisture equilibrium content
Ne	Total number of finite elements used in FE simulations
t	Time
V	Unit-cell total volume
$V^{(\alpha)}$	subcell volume
v_f	Fiber volume fraction
v_m	Matrix volume fraction
v_v	Void volume fraction
w	Width
w_f	Fiber weight fraction
w_m	Matrix weight fraction
w_v	Void weight fraction
$X^{(\alpha)}$	Subcell length in the flux direction
α	Subcell
ρ_{air}	Air density
ρ^e_v	Empty void's density
ρ^f_v	Fluid-filled void's density

ρ_m	Matrix density
ρ_{water}	Water density
$\boldsymbol{\varphi}$	Effective composite concentration gradient
$\boldsymbol{\varphi^{(\alpha)}}$	Subcell concentration gradient
$\varphi^{(\alpha)}_i$	Concentration gradient in direction i through the subcell α
φ_i	Homogenized concentration gradient through the composite in direction i

Introduction

Knowing long-term properties of composites is important when the materials shall be used in critical applications that are exposed to various environmental conditions. This topic is important for marine applications[1, 2], oil & gas industry[3], aerospace industry[4, 5] and others. The long-term properties are typically dependent on mechanical loading and environmental conditions (temperature, moisture, oxidation, etc.). Particularly, the effect of fluid concentration on the mechanical properties of polymeric composites has been discussed by Weitsman and Elahi[6]. This paper concentrates on the diffusion of water, as the environment, through the fiber reinforced polymer (FRP) composites, focusing on experimental, analytical, and numerical studies.

The traditional approach to obtain long-term mechanical properties of material in water is to saturate the material in water and to measure the mechanical properties subsequently[6-9]. Using this approach gives dry and fully saturated properties, obtaining the extreme conditions. However, it takes very long time for the water to diffuse into the composite. For thick walled structures, such as hulls of ships or some high-pressure pipelines, the water may never penetrate the entire thickness of the laminate, causing a gradient of water concentration in the composite. In order to obtain better predictions of the long-term properties, a more accurate knowledge of the concentration profiles of the water in

the laminate needs to be known. It should also be noted that a gradient of water in the laminate can cause internal stresses altering the strength of the material, when compared to the ones measured in totally dry or wet conditions[10].

The water uptake can be calculated if the diffusivity is known. Measurement methods for diffusivity of isotropic polymers, following the Fickian diffusion, are well established. The typical method is given by ASTM D5229[11]. When a very thin specimen is considered for the immersion test, e.g., 150x150x1.5 mm, following the ASTM D5229–92(04) without sealing the edges, the diffusion process can be approximated by 1-D diffusion through the thickness. Eq. (1) links the mass uptake to diffusivity from solving the 1-D Fickian diffusion equation, as described in[12]:

$$M(t) = M_\infty \left[1 - \left(\frac{8}{\pi^2}\right) \sum_{i=0}^{\infty} \frac{e^{-(2i+1)^2 \left(\frac{\pi}{h}\right)^2 D_\perp t}}{(2i+1)^2}\right] \quad (1)$$

By fitting the exact solution of the diffusion equation to an exponential function, the ASTM standard simplifies Eq. (1) to:

$$M(t) = M_\infty \left[1 - \exp\left(-7.3 \left(\frac{D_\perp t}{h^2}\right)^{0.75}\right)\right] \quad (2)$$

where M(t) is the water content, M_∞ is the water saturation content, *t* is time, h is the thickness and $D_\perp$ the diffusivity in the thickness direction of the plate.

When dealing with isotropic materials having complex geometries it is possible to predict water diffusion by numerically solving the governing differential equation either using finite difference or finite element method. For immersed epoxy and vinylester, Fan et al.[13], determined water concentration in each element with the finite difference method by a weighed average of the nodal concentrations surrounding the element. The water

concentration in the specimen was determined by the accumulated concentration from all elements in the body.

The diffusivity of an orthotropic composite ply is anisotropic[14]. The diffusivity along the fibers is different from the diffusivity across the fibers. The standard method for obtaining diffusivity for a composite ply is the same as for polymers. A flat sample is made, the edges are sealed, the sample is fully immersed in fluid and the diffusivity from the Fickian model is calculated using Eq. (1) or Eq. (2).

The approach works well for obtaining the through thickness diffusivity, because regular thin plies or laminates can be tested. Sealing the edges remains to be a challenge though. It is usually assumed that the through thickness diffusivity and in-plane diffusivity across the fibers are the same. This is a good assumption for transversely isotropic materials. The diffusivity in fiber direction is more difficult to obtain. Using a standard thin laminate is not well suited for measuring diffusivity in the fiber direction. The large surface area would have to be sealed and it would take a long time for water to get into the specimen. Making very thick specimens and cutting them in a way that the fiber ends are forming the large surface has solved the problem[15-19]. This is described in detail in the experimental methods. In this paper, the testing for the composites was done with open edges and diffusivity was calculated with a 3-D approach. This method was shown to be the most rigorous by Arnold et al. [18].

The glass fibers themselves are often seen as non-permeable to water, assuming to have zero diffusivity. Several experimental investigations of moisture diffusion in fiber-reinforced polymer composites have suggested different diffusions along the fiber

direction and perpendicular to the fiber direction[20, 21]. The diffusivity along the fiber direction can be 2-4 times larger than the transverse diffusivity for glass fiber laminates[20, 22] and about 14 times higher for carbon fiber rods[23]. Taking into consideration the anisotropy of the fiber-reinforced composites, Shen and Springer[14] formulated a relationship between the diffusivity of matrix, diffusivity of fibers, fiber volume fraction and fiber orientation in order to determine the diffusivity of composites in the lateral (across) fiber direction. The idea is based on an analogy between moisture diffusion and thermal conduction[24]. The model has been widely applied in capturing the moisture diffusion in FRP composites[25, 26]. Several theories were developed to predict anisotropic diffusivity based on the diffusivity of the matrix and the geometrical arrangement of the fibers[14, 22]. Shen and Springer[14] proposed an expression to predict transverse and parallel diffusivity from matrix diffusion. A comparison of micromechanical analytical models has been reported by Bao and Yee [16]. It is noted that several experimental studies have shown that typical diffusivity of the FRP composites in the transverse direction is around 1.5-3 times lower than the diffusivity of the corresponding resin, e.g. Bond[21]. Experimental investigations mentioned above have shown that diffusivity along the fiber direction can be 2-14 times higher than the one in the transverse direction. In this situation, it is clear that the diffusivity in FRP composite cannot be adequately captured by considering only matrix and fiber constituents, with zero diffusivity for the fiber. Rocha et al.[22] proposed a FE model with high diffusivity interphase, in order to explain anisotropic diffusivity in composites. They concluded that the fiber barrier effect is partly responsible for the anisotropic diffusion in composites, but this alone does not explain the effect observed. For the system investigated here the

existing theories could not predict the anisotropic behavior found experimentally and a new approach had to be developed for describing the diffusion along and across fiber directions.

Humeau et al.[27], performed computed tomography scans of GF/epoxy samples and observed that voids are elongated in the fiber direction. However, they reported that the anisotropy in diffusivity of samples without voids was as great as for the samples with voids, and concluded that voids elongation could not explain the anisotropic diffusion behavior.

In this this work, 3-D diffusion has been studied experimentally using samples with fibers oriented in different directions. The effect of voids on the moisture saturation content has been studied theoretically and experimentally. The orthotropic diffusion constants have been obtained from the experiments using 3-D anisotropic diffusion theory. Finally, a micromechanical approach has been developed where fiber bundles are modelled as anisotropic.

Materials and methods

Materials

A typical glass fiber epoxy used for wind turbine and marine applications was selected for this study. The glass fibers were HiPer-Tex™ unidirectional (UD) fabrics from 3B having average radius 9 μm and density 2.5 g/cm^3. The epoxy used was Hexion™ RIMR135™ resin and RIMH137™ hardener mixed with a mass ratio of 100:30. The glass transition temperature of the resin is 84.7°C, the curing temperature 80°C and its

density is 1.2 g/cm^3 [28]. A thick laminate was made by vacuum assisted resin infusion of 80 plies resulting in an average ply thickness of 0.85 mm. Samples were cut from this laminate using a water-cooled diamond saw in order to obtain samples with fibers parallel and transverse to the surface, as shown in Fig. 1.

[Insert Fig.1]

Fig.1. Composite samples configurations. Dimensions are 50 mm x 50 mm x 1.5 mm.

For each of the configurations in Fig. 1, four samples having dimensions 50 x 50 mm were cut with a water cooled diamond saw, machined to a thickness of 1.5 mm and grinded with sandpaper having grit 800, in order to avoid erroneous weight gain measurements[22].

Experimental methods

Fiber volume fractions were obtained by burn off tests and density measurements. The burn off test, was performed following ASTM Standard D3171[29]. The volume fraction obtained experimentally was 59.5%. The difference between volume fraction obtained by burn off test and by density measurement was only 0.2%.

In order to obtain also the matrix diffusion constants a set of 4 neat resin samples was obtained by resin molding and degassing, in order to eliminate the potential voids caused by molding. Similar to the glass-fiber epoxy samples, four neat resin samples having dimensions 50 x 50 x 1.5 mm were obtained by cutting with a water-cooled diamond saw, machining and grinding using 800 grit sandpaper.

All samples were cured at room temperature for 24 hours and post-cured in an oven at 80°C for 12 hours, according to the manufacturer's recommendations. Before conditioning the samples were dried at 60°C for 72 h in an oven, monitoring their weight until no substantial weight change occurred. The curing process and the long time drying at 60°C ensure that complete curing occurs for both neat resin and composite samples. The samples are shown in Fig. 2.

[Insert Fig.2]

Fig.2. Samples used for the diffusion experiment.

The void volume fraction in the laminate was measured by image analysis of optical microscope images, opportunely converted in black and white, Fig. 3.

[Insert Fig.3]

Fig.3. (a) Optical microscope image showing voids; **(b)** converted black and white threshold image used for void volume fraction evaluation.

The void volume fraction was obtained by analysis of the image color histogram, and resulted in 0.44 % ± 0.32%. Fig. 4 shows the micrographs of the FRP composite at different normal directions: longitudinal fiber and transverse fiber directions.

[Insert Fig.4]

Fig. 4. (a) Laminate coordinate system; **(b)** intra-bundle void in the 2-3 plane; **(c)** intra-bundle void in the 1-3 plane.

A conditioning chamber was made by filling a thermally insulated bucket with distilled water. An electrical resistance was placed in the bucket together with a thermocouple, in order to have a constant temperature of 60°C ± 1°C. An aluminum sample holder was used for keeping the samples in a vertical position and expose all flat faces to water. Samples mass was measured regularly with a Mettler Toledo AG204 DeltaRange scale, having a sensitivity of 0.1 mg and a capacity of 61 g. They were removed from the conditioning chamber 4 at a time, their surfaces dried with a cloth and weighed immediately, in order to prevent water from diffusing out of the samples.

All specimens had open edges. In order to enforce 1-D flow conditions in a diffusion experiment it is good practice to maximize the width to thickness ratio of the samples or to seal the edges with stainless steel. The sealant is often glued to the small surface of the samples' edges. This glue may absorb water, influencing the measurement, or, even worst, fall off from the sample during the experiment. It was therefore decided to keep open the edges of all samples, as the width to thickness ratio was quite big: 33. Saturation was measured up to 506 hours, when the weight gain curve had flattened out.

Modeling diffusion in FRP composites

Diffusivities of water in a polymer or composite can be obtained from measuring the water uptake with time. One approach is to simply measure the macroscopic diffusivities in the principal orthotropic directions of the material. This approach will be described first for the simple 1-D case and the better 3-D approach. It is a relatively simple method

sufficient for characterizing the diffusion behavior. An engineer who wants to determine the concentration profile of water within a component made of FRP composites would not need any additional information, provided the diffusion in FRP composites can be modeled as Fickian diffusion. The second approach explains diffusivity from the micromechanics point of view, which gives insights into the reasons for anisotropic diffusion behavior.

Macroscopic model

The 1-D water uptake from the macroscopic diffusion through the specimen thickness can be described by the method given in the ASTM Standard[11], as written in Eq. (1). If the diffusivity of a composite laminate is measured, this diffusivity obtained is typically in the direction perpendicular to the fibers. When knowing the specimen dimensions and the saturation level of the water uptake, the diffusivity $D_{\perp}$ can be found by obtaining the best fit for the mass uptake data vs. time using Eq. (3). In the above equation, the effect of volumetric changes (swelling) during the diffusion process is neglected. In some polymers immersed in water, a relatively small volume change can cause deviation from the Fickian diffusion[13].

The above method is based on the 1-D diffusion and requires the edges of the samples to be sealed. Sealing the edges with a diffusion-tight material can be difficult. Often metal foils are used, but they sometimes do not bond easily to the polymer. When the foils fall off during the experiment, the data can be severely disturbed. A simpler way to measure diffusivity of anisotropic composites is to make samples without sealing the edges. In that

case a 3-D version of Eq. (1) is needed. The 3-D solution to mass uptake in an anisotropic plate, following the Fickian diffusion, was reported by Crank[12]:

$$M(t) = M_\infty \left[1 - \left(\frac{8}{\pi^2}\right)^3 \sum_{i=0}^{\infty}\sum_{j=0}^{\infty}\sum_{k=0}^{\infty} \frac{e^{-(2i+1)^2\left(\frac{\pi}{h}\right)^2 D_\perp t}}{(2i+1)^2} \frac{e^{-(2j+1)^2\left(\frac{\pi}{w}\right)^2 D_\perp t}}{(2j+1)^2} \frac{e^{-(2k+1)^2\left(\frac{\pi}{l}\right)^2 D_\parallel t}}{(2k+1)^2}\right] \quad (3)$$

where l is the sample length, w its width, $D_\perp$ the laminate diffusivity in the direction perpendicular to the fibers and $D_\parallel$ the laminate diffusivity in the direction parallel to the fibers, as shown in Fig. 5.

[Insert Fig.5]

Fig. 5. Configuration of samples used for parallel and transverse diffusion measurement.

For the composite samples with transverse configuration, Eq. (3) can be used, while for the samples with parallel configuration, Eq. (3) must be modified to take into account for the diffusion in the direction parallel to the fibers going through the thickness, as follows:

$$M(t) = M_\infty \left[1 - \left(\frac{8}{\pi^2}\right)^3 \sum_{i=0}^{\infty}\sum_{j=0}^{\infty}\sum_{k=0}^{\infty} \frac{e^{-(2i+1)^2\left(\frac{\pi}{h}\right)^2 D_\parallel t}}{(2i+1)^2} \frac{e^{-(2j+1)^2\left(\frac{\pi}{w}\right)^2 D_\perp t}}{(2j+1)^2} \frac{e^{-(2k+1)^2\left(\frac{\pi}{l}\right)^2 D_\perp t}}{(2k+1)^2}\right] \quad (4)$$

Fig. 5 shows the diffusivities for each direction in both transverse and parallel configuration. For the neat resin, due to the assumption of isotropy $D_\perp = D_\parallel = D_M$. Eq. (3) becomes:

$$M(t) = M_\infty \left[1 - \left(\frac{8}{\pi^2}\right)^3 \sum_{i=0}^{\infty}\sum_{j=0}^{\infty}\sum_{k=0}^{\infty} \frac{e^{-(2i+1)^2\left(\frac{\pi}{h}\right)^2 D_M t}}{(2i+1)^2} \frac{e^{-(2j+1)^2\left(\frac{\pi}{w}\right)^2 D_M t}}{(2j+1)^2} \frac{e^{-(2k+1)^2\left(\frac{\pi}{l}\right)^2 D_M t}}{(2k+1)^2}\right] \quad (5)$$

where D_M is the matrix diffusivity.

Microscopic model

The anisotropic diffusivity can also be predicted by using a micromechanics model based on mainly the diffusivities of the resin and fiber bundles in the composite. A micromechanics model is formulated to determine the overall (homogenized) anisotropic diffusivity of FRP composites, comprising of unidirectional fibers embedded in matrix. The micromechanics model is based on a simple unit-cell with four fiber and matrix subcells, as depicted in Fig. 6.

[Insert Fig.6]

Fig. 6. A simplified microstructure of FRP composite.

This unit-cell model has been successfully used to determine the mechanical and non-mechanical response of FRP composites, such as thermo-viscoelastic, piezoelectric, and heat conduction behaviors[30, 31]. The first subcell is the fiber constituent and the remaining subcells are matrix. It is noted here that the fiber constituent in case of typical FRP composite is actually a fiber bundle that consists of fiber filaments, as shown in Fig. 4. Thus, fluid can penetrate within the filaments inside the fiber bundle, which might explain the relatively high diffusivity along the fiber direction in FRP composites. Perfect bonding at the interphases between the fiber bundle and matrix is assumed, and a periodic boundary condition is imposed on the unit-cell.

In determining the diffusivity of the composite, it is also assumed that volumetric expansion (swelling) is negligible, thus both fiber and matrix diffusion behaviors follow

the Fickian diffusion. The flux of the fluid that passed through the homogenized composite faces, $\bar{\mathbf{f}}$, is formulated based on the volume average of the flux in the four subcells:

$$\bar{\mathbf{f}} = \frac{1}{V}\sum_{\alpha=1}^{4}\mathbf{f}^{(\alpha)}\left(\mathbf{X}^{(\alpha)}\right)dV^{(\alpha)} \approx \frac{1}{V}\sum_{\alpha=1}^{4}V^{(\alpha)}\mathbf{f}^{(\alpha)} \quad (6)$$

where $\mathbf{f}^{(\alpha)}$ and $V^{(\alpha)}$ are the flux and volume of subcell (α), respectively, and and $\mathbf{X}^{(\alpha)}$ is the spatial location of each point within the unit-cell. It is also assumed that field variables within one subcell are uniformly distributed. A total volume of the unit-cell is $V = \sum_{\alpha=1}^{4}V^{(\alpha)}$. When the fiber volume fraction is considered, then $V = \sum_{\alpha=1}^{4}V^{(\alpha)}=1$. The flux in the composite is formed due to the gradient of fluid concentration and a linear relation is considered between the flux and concentration gradient in the homogenized composite:

$$\bar{\mathbf{f}} = -\bar{\mathbf{D}}\,\bar{\boldsymbol{\varphi}}; \quad \bar{\boldsymbol{\varphi}} = grad(C) \quad (7)$$

Here $\bar{\mathbf{D}}$ and $\bar{\boldsymbol{\varphi}}$ are the effective diffusivity and concentration gradient of the homogenized composite, respectively, and C is the water concentration in the homogenized composite which is time and spatial dependent. The concentration gradient of the homogenized composite is related to the concentration gradient of each subcell by formulating a concentration matrix for each subcell $\mathbf{B}^{(\alpha)}$. The idea of formulating the concentration matrix to relate the field variables of the constituents to the field variable of the composite was originally proposed by Hill[32] for a linear elastic response of composites. The concentration gradient in each subcell is given by:

$$\boldsymbol{\varphi}^{(\alpha)} = \mathbf{B}^{(\alpha)}\bar{\boldsymbol{\varphi}} \quad (8)$$

A linear relation like in Eq. (7) is adopted for the constitutive relation in each subcell:

$$\mathbf{f}^{(\alpha)} = -\mathbf{D}^{(\alpha)}\boldsymbol{\varphi}^{(\alpha)} \tag{9}$$

where $\mathbf{D}^{(\alpha)}$ is the subcell diffusivity. Substituting Eq. (8) into Eq. (9) gives:

$$\mathbf{f}^{(\alpha)} = -\mathbf{D}^{(\alpha)}\mathbf{B}^{(\alpha)}\bar{\boldsymbol{\varphi}} \tag{10}$$

Substituting Eq. (10) into Eq. (6) gives the effective flux in terms of diffusivity properties of the constituents and volume content:

$$\bar{\mathbf{f}} \approx -\frac{1}{V}\sum_{\alpha=1}^{4} V^{(\alpha)}\mathbf{D}^{(\alpha)}\mathbf{B}^{(\alpha)}\bar{\boldsymbol{\varphi}} \tag{11}$$

Finally, the effective diffusivity of the composite is determined by comparing Eq. (7) and Eq. (11):

$$\bar{\mathbf{D}} = \frac{1}{V}\sum_{\alpha=1}^{4} V^{(\alpha)}\mathbf{D}^{(\alpha)}\mathbf{B}^{(\alpha)} \tag{12}$$

The conservation of mass of the fluid in the composite body leads to:

$$\frac{dC}{dt} = -Div(\bar{\mathbf{f}}) \tag{13}$$

where *t* denotes the time variable.

In order to determine the diffusion behaviour and diffusivity of the homogenized composite, micromechanical relations between the subcells need to be obtained. Consider a unit-cell model in Fig. 6 placed in the Cartesian coordinate, with fibers are aligned in 1 direction, and 2 and 3 are the directions lateral and transverse to the fiber composite. The flux and water concentration along the fiber direction are expressed as:

$$V^{(1)}f_1^{(1)} + V^{(2)}f_1^{(2)} + V^{(3)}f_1^{(3)} + V^{(4)}f_1^{(4)} = \bar{f}_1 \tag{14}$$

$$\varphi_1^{(1)} = \varphi_1^{(2)} = \varphi_1^{(3)} = \varphi_1^{(4)} = \bar{\varphi}_1 \tag{15}$$

The flux and water concentration across the fiber direction are expressed as:

$$f_2^{(1)} = f_2^{(2)} \quad (16)$$

$$f_2^{(3)} = f_2^{(2)} \quad (17)$$

$$\frac{V^{(1)}}{V^{(1)}+V^{(2)}}\varphi_2^{(1)} + \frac{V^{(2)}}{V^{(1)}+V^{(2)}}\varphi_2^{(2)} = \bar{\varphi}_2 \quad (18)$$

$$\frac{V^{(3)}}{V^{(3)}+V^{(4)}}\varphi_2^{(3)} + \frac{V^{(4)}}{V^{(3)}+V^{(4)}}\varphi_2^{(4)} = \bar{\varphi}_2 \quad (19)$$

$$f_3^{(1)} = f_3^{(3)} \quad (20)$$

$$f_3^{(2)} = f_3^{(4)} \quad (21)$$

$$\frac{V^{(1)}}{V^{(1)}+V^{(3)}}\varphi_3^{(1)} + \frac{V^{(3)}}{V^{(1)}+V^{(3)}}\varphi_3^{(2)} = \bar{\varphi}_3 \quad (22)$$

$$\frac{V^{(2)}}{V^{(2)}+V^{(4)}}\varphi_3^{(3)} + \frac{V^{(4)}}{V^{(2)}+V^{(4)}}\varphi_3^{(4)} = \bar{\varphi}_3 \quad (23)$$

Using the micromechanical relations, Eqs. (14)-(23) and constitutive relations for the constituents in Eq. (9), the concentration matrix for each subcell can be obtained. Finally, the effective diffusivity is determined from Eq. (12). In this study, the fiber bundle is assumed transversely isotropic and the polymeric matrix is considered isotropic with regards to their diffusion behaviors. The fiber diffusivity is $\mathbf{D}^{(f)}$ =diag($D_{11}^{(f)}$, $D_{22}^{(f)}$, $D_{22}^{(f)}$), while the diffusivity of matrix is $\mathbf{D}^{(m)} = D^{(m)}\,\mathbf{I}_3$, where $\mathbf{I}_3$ is the identity matrix. The diffusivity of the composite is given as:

$$\bar{\boldsymbol{D}} = diag(\bar{D}_{11}, \bar{D}_{22}, \bar{D}_{33});\ \ \bar{D}_{33} = \bar{D}_{22} \quad (24)$$

$$\bar{D}_{11} = \frac{1}{V}\left(V^{(1)}D_{11}^{(f)} + V^{(2)}D^{(m)} + V^{(3)}D^{(m)} + V^{(4)}D^{(m)}\right) \quad (25)$$

$$\bar{D}_{22} = \frac{1}{V}\left(V^{(1)}\frac{D^{(m)}D_{22}^{(f)}(V^{(1)}+V^{(2)})}{V^{(1)}D^{(m)}+V^{(2)}D_{22}^{(f)}} + V^{(2)}\frac{D^{(m)}D_{22}^{(f)}(V^{(1)}+V^{(2)})}{V^{(1)}D^{(m)}+V^{(2)}D_{22}^{(f)}} + V^{(3)}D^{(m)} + V^{(3)}D^{(m)}\right) \quad (26)$$

In order to solve for the governing equation in Eq. (13), the finite element (FE) method is used and the constitutive relation in Eq. (11) is implemented at each Gaussian point within continuum 3-D elements. Each continuum element has eight nodes. The concentration of the fluid is evaluated at the nodes. The total amount of fluid concentration in the composite during the diffusion process is determined as follows;

$$C(t) = \frac{1}{V}\sum_{m=1}^{Ne} C^{(m)}\Delta V^{(m)}\,; \quad C^{(m)} = \frac{1}{8}\sum_{i=1}^{8} C_i^{(m)} \tag{27}$$

where *Ne* is total number of finite elements used in solving the diffusion equation in the composite body. The amount of fluid concentration at each instant of time in Eq. (27) is correlated to the fluid concentration obtained from experiment. The total fluid concentration is related to the fluid uptake as follow:

$$C(t) = \frac{M(t)}{M_\infty} \tag{28}$$

The micromechanics model is implemented in a continuum three-dimensional finite element. At each Gaussian integration point within the element, the constitutive model for the diffusion behavior is determined from the micromechanics model. In this study the user material subroutine within ABAQUS commercial FE, written in Fortran, is used to integrate the micromechanics model to FE analyses. For the post-processing, the total amount of fluid in the composites is determined by integrating the field variables at the nodes obtained from the FE analyses. For this purpose a Matlab code was generated for reading the nodal field variables and numerically integrating them to obtain the overall fluid concentration.

In order to simulate the fluid sorption mimicking the FRP and resin specimens, finite element meshes with 8 node hexahedral elements were generated for the plate with dimension 50x50x1.5mm. A convergence study was first conducted in order to determine sufficient numbers of elements by comparing the overall fluid concentration to the

analytical solution of isotropic diffusion in resin. In this study, a total of 4000 elements was sufficient in capturing the fluid sorption response. Fig. 7 shows the FE meshes.

[Insert Fig.7]

Fig. 7. Mesh used for the FE analysis.

Results

Diffusivity of the matrix

The weight increase at saturation is about 3.18 %. Saturation has been defined as the moment when the difference in two consecutive measurements is lower than 0.5%. The diffusivity of the matrix can be easily obtained for an isotropic polymer, by fitting the experimental results to the 1-D diffusion solution in Eq. (1), for the hypothesis of an infinitely wide plate (a very thin plate). Alternatively, it is possible to use 3-D diffusion solution in Eq. (5), where all diffusion constants are set equal to D_M. The use of Eq. (5) instead of the 1-D flow equation, Eq. (1), yields more accurate prediction of the diffusion constant because it accounts for both the finite width of the laminate and the diffusion flow through its edges. The experimental results are compared with both Eq. (1) and Eq. (5), in Fig. 8 and Fig. 9 respectively. In Fig. 8 the results are fitted using Eq. (1), valid for 1-D diffusion in an infinitely wide plate. The matrix diffusivity obtained is 0.0068 mm^2/h ($1.89\ 10^{-6}$ mm^2/s).

[Insert Fig.8]

Fig. 8. Water uptake measured as % weight increase vs. time in hours. 1-D model.

In Fig. 9 is reported the fit between experimental measurements and Eq. (5), valid for 3-D diffusion in plates of finite width.

[Insert Fig.9]

Fig. 9. Water uptake measured as % weight increase vs. time in hours. 3-D model.

The diffusivity obtained by the 3D method described above is 0.0063 mm^2/h (1.75 10^{-6} mm^2/s). The 1-D diffusion equation, yields a higher diffusivity prediction than the 3-D diffusion equation, as it does not consider the edge effects as a cause for steeper weight gain curve. The difference is quite small, 7.4 %

Saturation level of the composite

The saturation level of the neat resin obtained experimentally is 3.18%. The saturation level of the composite, assuming that no voids are present in the material can be obtained by [7]:

$$M_\infty^C = M_\infty^M \left(1 - w_f\right) = M_\infty^M \frac{(1-v_f)\rho_m}{v_f\rho_f + (1-v_f)\rho_m} = 0.774\ \% \qquad (29)$$

where w_f is the fiber weight fraction, v_f the fiber volume fraction, ρ_m the matrix density, ρ_f the fiber density, and M_∞^M= 3.18 % the matrix saturation moisture content. The predicted moisture saturation content, 0.774% is far from the result observed experimentally: 0.96%. This difference could be due to the presence of voids in the laminate.

It is possible to extend Eq. (29) in order to take into account for the presence of voids:

$$M_\infty = M_\infty^M\, w_m + M_\infty^V\, w_v = \frac{M_\infty^M\, v_m\, \rho_m + M_\infty^V\, v_v\, \rho_v^f}{v_f\rho_f + v_m\rho_m + v_v\, \rho_v^e} \qquad (30)$$

where w_m is the matrix weight fraction, w_v is the void weight fraction, M_∞^M= 3.18 % the matrix saturation moisture content, M_∞^V= 100 % the void saturation moisture content, v_f the fiber volume fraction, v_m the matrix volume fraction, v_v the void volume fraction, ρ_f the fiber density, ρ_m the matrix density, ρ_v^f the filled void's density and ρ_v^e the empty void's density.

We impose volume and mass conservation, Eq. (31). We also define void density as equal to water density when filled and as equal to air density when empty, Eq. (32).

$$v_f + v_m + v_v = 1 \quad ; \quad w_f + w_m + w_v = 1 \tag{31}$$

$$\rho_v^f = \rho_{water} \quad ; \quad \rho_v^e = \rho_{air} \cong 0 \tag{32}$$

where ρ_{water} is water density and ρ_{air} is air density. We simplify $\rho_{air} \approx 0$.

Eq. (30) becomes therefore:

$$M_\infty = \frac{M_\infty^M \, v_m \, \rho_m + M_\infty^V \, v_v \, \rho_{water}}{v_f \rho_f + v_m \rho_m} \tag{33}$$

The void volume fraction of the laminate was 0.44 %, the composite predicted saturation content is therefore 0.99 %, very close to the value obtained experimentally: 0.96 % (only 3% deviation).

Diffusivity of the composite along and across the fiber direction

The diffusivities of the composite in the transverse and parallel directions were computed using both 1-D and 3-D diffusion models. The saturation level used was 0.96% for both sample configurations.

In Fig. 10 (a) and (b) the experimental results are fitted using 1-D diffusion equation, Eq. (1). The diffusivity constants obtained are 0.0051 mm^2/h (1.42 10^{-6} mm^2/s) for transverse diffusion and 0.021 mm^2/h (5.83 10^{-6} mm^2/s) for parallel diffusion.

[Insert Fig.10]

Fig. 10. Water uptake measured as % weight increase vs. time in hours, fitted with the 1-D equation.

In Fig. 11 (a) and (b), diffusivity was obtained by simultaneous fitting of transverse samples and parallel samples weight gain curves with Eqs. (4) and (5) respectively.

[Insert Fig.11]

Fig. 11. Water uptake measured as % weight increase vs. time in hours, fitted with the 3-D equation.

The regression was done using non-linear least squares method. The fit is easily performed as the weight gain curve of the transverse samples is dominated by the ply transverse diffusivity $D_\perp$ and the weight gain curve of the parallel samples is dominated by the ply parallel diffusivity, $D_\parallel$. The transverse diffusivity obtained is 0.0045 mm^2/h (1.25 10^{-6} mm^2/s) and the parallel diffusivity obtained is 0.02 mm^2/h (5.56 10^{-6} mm^2/s). Hence the parallel diffusivity obtained is 4.44 times higher than the transverse diffusivity. Similar to the neat resin diffusivity, we observe that also in this case, the 1-D diffusion equation predicts higher diffusivity compared to the 3-D diffusion equation, both for

transverse diffusivity (11.8 %) and parallel diffusivity (4.8 %). One of the reasons for this difference is the finite width of the sample that is taken into account by Eqs. (3) and (4). It is interesting to observe that for the transverse diffusion the deviation between 1-D diffusion results and 3-D diffusion results is higher than for parallel diffusion. This is because the 1-D diffusion results neglect the flow through the edges, which runs in the direction parallel to the fibers, and has therefore 4.44 times higher diffusivity. For the parallel diffusion, the difference between results obtained by 1-D and 3-D diffusion equations is smaller, because the diffusion through the edges occurs in the direction transverse to the fibers, and is therefore slower than the diffusion in the thickness direction, that runs parallel to the fibers. The results of the diffusivities characterized using macroscopic analytical model are summarized in Table 1.

[Insert Table 1]

Table 1. Diffusivities obtained for neat resin and composite using 1-D and 3-D diffusion equation.

Diffusion analyses using the micromechanical model

As discussed in Section 3, a micromechanical model, which is implemented in FE analysis, is presented for determining the homogenized diffusion behavior in FRP composites. The main advantages of using the homogenization approach are that it can be used to easily determine anisotropic diffusivities of FRP with different fiber volume

contents while incorporating different diffusivities of fiber bundle and matrix, making it easy for material selections with desired diffusion performance, it permits predictions of the diffusion behavior in laminated composites with different fiber orientations, and it allows performing diffusion of FRP structures with more complex geometries and boundary conditions.

In order to test the micromechanics and numerical methods, the diffusion constant of the resin was first determined, both from the 1-D and 3-D analyses. In the 3-D analysis, the micromechanics model was considered by setting the fiber volume content to zero. The diffusivity of resin from the 1-D analysis is 0.0067 mm^2/h ($1.86\ 10^{-6}$ mm^2/s), and the one from the 3-D analysis is 0.0062 mm^2/h ($1.71\ 10^{-7}$ mm^2/s). These values are very close to the analytical solutions discussed above. The concentration of water during the diffusion process is shown in Fig. 12.

[Insert Fig.12]

Fig. 12. Concentration of water in the resin from the micromechanics and numerical analyses.

The micromechanics model is now used to determine the anisotropic diffusivity of fiber bundles in the FRP composites. Prior to determining the diffusivities of fiber bundles in the longitudinal and lateral directions using the micromechanics model, parametric studies were considered, see Appendix. From the analyses, the diffusivity of the fiber bundle in the lateral direction is $D_{22}^{(f)}$= 0.0031 mm^2/h ($0.86\ 10^{-6}$ mm^2/s), while the one in the longitudinal direction is $D_{11}^{(f)}$= 0.0308 mm^2/h ($8.55\ 10^{-6}$ mm^2/s). The diffusivity of the

fiber bundle along the longitudinal direction is much higher than the diffusivity of fiber bundle in the lateral direction, and also higher than the diffusivity of matrix. Fig. 13 (a) and (b) shows the diffusion behavior in FRP composites, tested transverse and parallel to the longitudinal fiber direction. From the micromechanics analyses, the effective diffusivities can be easily determined from Eq. (26) and Eq. (27). The overall diffusivities of the FRP with 59.5 % fiber volume content are: $\overline{D}_{11}$= 0.021 mm^2/h (5.80 10^{-6} mm^2/s) and $\overline{D}_{22}$= 0.0042 mm^2/h (1.16 10^{-6} mm^2/s), which are summarized in Table 1.

[Insert Fig.13]

Fig. 13. Micromechanics analyses of the diffusion in FRP composites (a) transverse direction, (b) parallel direction.

Discussion

Measuring the diffusivity of a solid immersed in a fluid is typically done by exposing specimens with sealed edges to a fluid and measuring the weight gain. A simple 1-D formula stated in ASTM D5229[(11)] is often used to calculate the diffusivity. Testing with sealed edges is experimentally difficult; as the sealant may not bond properly giving distorted results. Performing tests with open edges and using 3-D diffusivity equations makes the testing much easier. The diffusivity is found by obtaining the best fit of the 3-D equation against the experimental data. The process is not as easy as just looking at the slope of the curve in the ASTM approach, but the best fit can be easily found using an optimization tool.

For the water uptake of neat resin and using thin plates the effect of the edges was small and using the 1-D or 3-D equation gave roughly the same results. It is recommended though to use the 3-D equation as it is more accurate and can also be used for thicker specimen geometries with more pronounced edge effects. The same can be said for measuring the water uptake of composite laminates.

Measuring diffusivity of composites in fiber direction is inherently difficult. Typical composite laminates are thin plates and the fibers are only exposed on one thin surface. Transverse diffusion dominates such samples. Making thick laminates can compensate the problem of a small exposed surface, but then the diffusion takes a long time. Making thick laminates and cutting thin slices creating thin specimens with a large exposed surface for fiber ends solved the problem and good measurements could be taken.

The small amount of voids causes an increase of the saturation level of the composite by 24 % (from 0.774% to 0.96%), and needs to be accounted for, since the saturation level is directly related to the diffusivity. Even a small void content has a large influence on the saturation level. However, voids are often distributed nonuniformly, making it complicated in determining the overall (average) response of composites by examining a representative microstructure of composites. The nonuniform distribution of voids also yields to localized fluid concentration within the composites.

For the glass fiber epoxy system investigated here, the diffusivity in the fiber direction was found to be about four times the diffusivity transverse to the fibers, see Table 1. This is a significant difference and anisotropic diffusion should be considered when calculating the fluid concentration profiles of structures and components. It is also noted that the diffusivity in the fiber direction is higher than the diffusivity of pure resin.

These results show that when considering only fiber bundle and matrix as constituents, the diffusivities of the fiber bundle cannot be assumed as zero, especially for the longitudinal fiber direction. However, assuming that individual glass fibers have 0 or very low diffusivity is often considered to predict diffusivity of the composite by knowing the diffusivity of the resin and geometric arrangement of the fibers. Using the assumption that fibers have zero or nearly zero diffusivity, e.g. the model developed by Shen and Springer [14] or the finite element based modes developed in [22], could not model the observed anisotropy. Several possible explanations to the above issue are as follows. This discrepancy is most likely because within fiber filaments in a single fiber bundle, resin and air pockets are present, which allow water to seep into fiber bundles. As a result, the net diffusivity of fiber bundle cannot be taken as zero. The glass fiber filaments themselves can be considered as zero or nearly zero permeability. However, considering that the fibers are arranged in bundles and the fibers are surrounded by a sizing (interface layer), diffusion channels may open up between fiber filaments and in the sizing. It is convenient to model this as diffusion within the fibers, but on a physical level another phase must be present that allows different diffusion than observed in the resin.

The presented micromechanics model could predict the observed global anisotropy by giving the fiber constituent (fiber bundle) an anisotropic diffusivity. The diffusivity across the fibers was less than that of the matrix and the diffusivity along the fibers was higher than the homogenized diffusivity of the materials. While the presented micromechanics approach seems to capture the anisotropy diffusivity in FRP composites with some rationale behind it, the detail mechanisms of the diffusion in FRP composites

are very complex and still not fully understood. From an engineering point of view, it is sufficient to accurately measure the anisotropic diffusion characteristics. From a materials point of view another phase allowing higher diffusivity must be present in the composite.

Conclusions

This study presents an experimental investigation and modeling of diffusion behavior in FRP composites. The experimental part considered thin specimens of pure resin and FRP composites with fibers arranged parallel and transverse to the thickness of the specimens. These specimens were immersed in distilled water, and moisture uptakes were monitored until saturation was reached. Specimens with unsealed edges were used, which is experimentally much easier than the standard approach of testing with sealed edges. The experimental results show that Fickian diffusion can be used to capture the diffusion process in these specimens. The experimental tests also showed that the existence of voids, although very small (around 0.44% volume content) can have a significant effect in the amount of water uptakes.

Two modeling approaches were considered in characterizing the diffusion behaviors of FRP composites, with the Fickian diffusion model. The first approach considers a phenomenological diffusion model and both 1-D and 3-D diffusion behaviors were considered. It was found that although the differences in the diffusivities characterized using 1-D and 3-D approaches are rather small, it is recommended to consider 3-D approach as it represents a more realistic condition. 1-D models are appropriate for samples

with sealed edges. It is noted that diffusivity of FRP composite along the fiber direction is 4.44 times the diffusivity in the transverse directions, indicating the anisotropic diffusion behaviors. The second approach is using a micromechanics model to capture the anisotropic diffusivity in FRP composites. Fiber bundle and matrix are taken as two constituents within the micromechanics model. The anisotropic diffusion behavior is captured by considering nonzero anisotropic diffusion coefficients for the fiber bundle and isotropic diffusion for the matrix. The rationale behind choosing nonzero diffusivity for the fiber bundle is due to occurrence of water seeping within fiber filament in the bundles during diffusion process.

Declaration of conflicting interests

The authors declared no potential conflicts of interest with respect to the research, authorship, and/or publication of this article.

Funding statement

The authors disclosed receipt of the following financial support for the research, authorship, and/or publication of this article: This work is part of the DNV GL led Joint Industry Project “Affordable Composites” with nine industrial partners and the Norwegian University of Science and Technology (NTNU). The authors would like to express their thanks for the financial support by The Research Council of Norway (Project 245606/E30 in the Petromaks 2 programme). The authors from Texas A&M University would like to acknowledge the funding supports from the National Science Foundation (CMMI-1266037) and Office of Naval Research (N00014-13-1-0604).

References

1. Durability of Composites in a Marine Environment. Dordrecht: Springer Netherlands, Dordrecht; 2014.
2. Davies P. Environmental degradation of composites for marine structures: new materials and new applications. Philosophical transactions Series A, Mathematical, physical, and engineering sciences. 2016;374(2071):20150272.
3. Ochoa OO, Salama MM. Offshore composites: Transition barriers to an enabling technology. Composites Science and Technology. 2005;65(15–16):2588-96.
4. Mouritz AP. Introduction to Aerospace Materials. Reston, VA: American Institute of Aeronautics and Astronautics ; Cambridge, UK : Woodhead Pub.; 2012.
5. Chamis CC, Singhal, S. N. Quantification of Uncertainties of Hot-Wet Composite Long Term Behavior. In: Thornton EA, editor. Aerospace Thermal Structures and Materials for a New Era. Progress in Astronautics and Aeronautics: American Institute of Aeronautics and Astronautics; 1995. p. 259-72.
6. Weitsman YJ, Elahi M. Effects of Fluids on the Deformation, Strength and Durability of Polymeric Composites – An Overview. Mechanics of Time-Dependent Materials. 2000;4(2):107-26.
7. Springer G. Environmental Effects on Composite Materials: Technomic Publishing Company; 1984.
8. Springer G. Environmental Effects on Composite Materials: CRC Press; 1984.
9. Weitsman YJ, SpringerLink. Fluid Effects in Polymers and Polymeric Composites: Springer US; 2012.
10. Jacquemin F, Fréour S, Guillén R. Prediction of local hygroscopic stresses for composite structures – Analytical and numerical micro-mechanical approaches. Composites Science and Technology. 2009;69(1):17-21.
11. Standard Test Method for Moisture Absorption Properties and Equilibrium Conditioning of Polymer Matrix Composite Materials. ASTM International; 2014.
12. Crank J. The mathematics of diffusion. Oxford: Clarendon Press; 1956.
13. Fan Y, Gomez A, Ferraro S, Pinto B, Muliana A, La Saponara V. The effects of temperatures and volumetric expansion on the diffusion of fluids through solid polymers. Journal of Applied Polymer Science. 2017;134(31):45151-n/a.
14. Shen CH, Springer G, Shen CH. Moisture absorption and desorption of composite materials. Journal of Composite Materials. 1976;10:2-20.
15. Choi HS, Ahn KJ, Nam JD, Chun HJ. Hygroscopic aspects of epoxy/carbon fiber composite laminates in aircraft environments. Composites Part A: Applied Science and Manufacturing. 2001;32(5):709-20.
16. Bao L-R, Yee AF. Moisture diffusion and hygrothermal aging in bismaleimide matrix carbon fiber composites—part I: uni-weave composites. Composites Science and Technology. 2002;62(16):2099-110.

17. Bao L-R, Yee AF. Moisture diffusion and hygrothermal aging in bismaleimide matrix carbon fiber composites: part II—woven and hybrid composites. Composites Science and Technology. 2002;62(16):2111-9.
18. Arnold JC, Alston SM, Korkees F. An assessment of methods to determine the directional moisture diffusion coefficients of composite materials. Composites Part A: Applied Science and Manufacturing. 2013;55(Supplement C):120-8.
19. Beringhier M, Simar A, Gigliotti M, Grandidier JC, Ammar-Khodja I. Identification of the orthotropic diffusion properties of RTM textile composites for aircraft applications. Composite Structures. 2016;137(Supplement C):33-43.
20. Blikstad M, Sjöblom POW, Johannesson TR. Long-Term Moisture Absorption in Graphite/Epoxy Angle-Ply Laminates. Journal of Composite Materials. 1984;18(1):32.
21. Bond DA. Moisture Diffusion in a Fiber-reinforced Composite: Part I - Non-Fickian Transport and the Effect of Fiber Spatial Distribution. Journal of Composite Materials. 2005;39(23):2113-41.
22. Rocha ICBM, Raijmaekers, Nijssen R. P. L., van der Meer F. P., Sluys, L. J. Experimental/numerical study of anisotropic water diffusion in glass/epoxy composites. 37th Risø International Symposium on Materials Science; Risø, Denmark: IOP Publishing Ltd; 2016.
23. Gagani A, Krauklis, A., Echtermeyer, A. T. Anisotropic fluid diffusion in carbon fiber reinforced composite rods: Experimental, analytical and numerical study. Manuscript submitted for publication. 2017.
24. Springer G, Tsai S, Springer G. Thermal conductivities of unidirectional materials (Thermal conductivities of unidirectional composite materials parallel and normal to filaments, using analogy to shear loading response). JOURNAL OF COMPOSITE MATERIALS. 1967;1:166-73.
25. Whitney JM. Three-Dimensional Moisture Diffusion in Laminated Composites. AIAA Journal. 1977;15(9):1356-8.
26. Loos AC, Springer G. S. MOISTURE ABSORPTION OF GRAPHITE-EPOXY COMPOSITES IMMERSED IN LIQUIDS AND IN HUMID AIR. J Compos Mater. 1979;13(2):131-47.
27. Humeau C, Davies P, Jacquemin F. Moisture diffusion under hydrostatic pressure in composites. Materials & Design. 2016;96:90-8.
28. HEXION. Technical Data Sheet. EPIKOTE Resin MGS RIMR 135 and EPIKURE Curing Agent MGS RIMH 137 2006.
29. Standard Test Methods for Constituent Content of Composite Materials. ASTM International; 2015.
30. Muliana AH, Kim JS. A two-scale homogenization framework for nonlinear effective thermal conductivity of laminated composites. Acta Mechanica. 2010;212(3):319-47.
31. Muliana AH. A micromechanical formulation for piezoelectric fiber composites with nonlinear and viscoelastic constituents. Acta Materialia. 2010;58(9):3332-44.
32. Hill R. Elastic properties of reinforced solids: some theoretical aspects. J Mech Phys Solids. 1963;11:357 to 72.

Appendix

This Appendix discusses parametric studies in examining the effect of anisotropic diffusion in the fiber bundles on the overall diffusion behaviors in FRP composites. The micromechanics model is used. The purpose of this parametric study is to guide the material parameter characterization, i.e., $D_{11}^{(f)}$, $D_{22}^{(f)}$ of the fiber bundles. The diffusivity of the isotropic matrix was obtained from the experimental test on neat resin. Fig. A1 illustrates the water uptake response in FRP parallel to the fiber axis. It is seen that the transverse diffusivity of the fiber bundle ($D_{22}^{(f)}$) has insignificant influence on the diffusion response in the parallel fiber direction. The diffusion in the parallel direction is governed by the axial diffusivity of the fiber, diffusion of the matrix, and fiber volume content. Fig. A2 shows the diffusion response along the transverse fiber direction. In this case, the transverse fiber diffusivity ($D_{22}^{(f)}$) has a significant effect while the axial fiber diffusivity ($D_{11}^{(f)}$) has insignificant effect, which is expected. This information can guide the determination of the anisotropic fiber diffusivity from the experimental data.

[Insert Fig.A1]

Fig. A1. Diffusion response of FRP in the parallel fiber direction: the effect of fiber anisotropy.

[Insert Fig.A2]

Fig. A2. Diffusion response of FRP in the transverse fiber direction: the effect of fiber anisotropy.

Highlights

- Micromechanical model for anisotropic diffusion in composites
- Testing procedure for the determination of anisotropic diffusion constants
- Prediction of moisture equilibrium content in the presence of voids

Figures

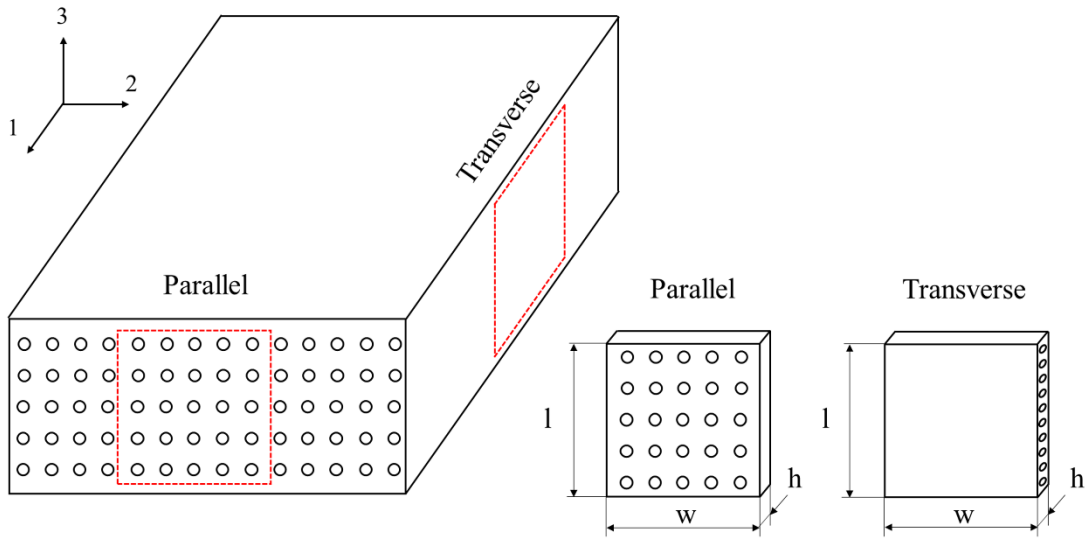

Fig.1. Composite samples configurations. Dimensions are 50 mm x 50 mm x 1.5 mm.

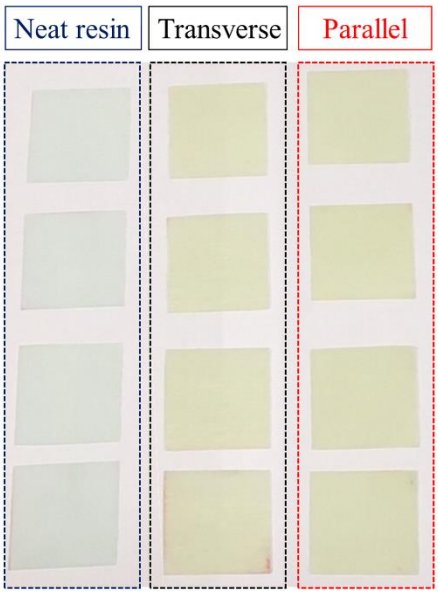

Fig.2. Samples used for the diffusion experiment.

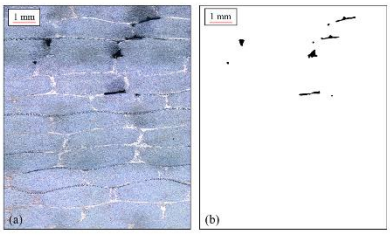

Fig.3. (a) Optical microscope image showing voids; **(b)** converted black and white threshold image used for void volume fraction evaluation.

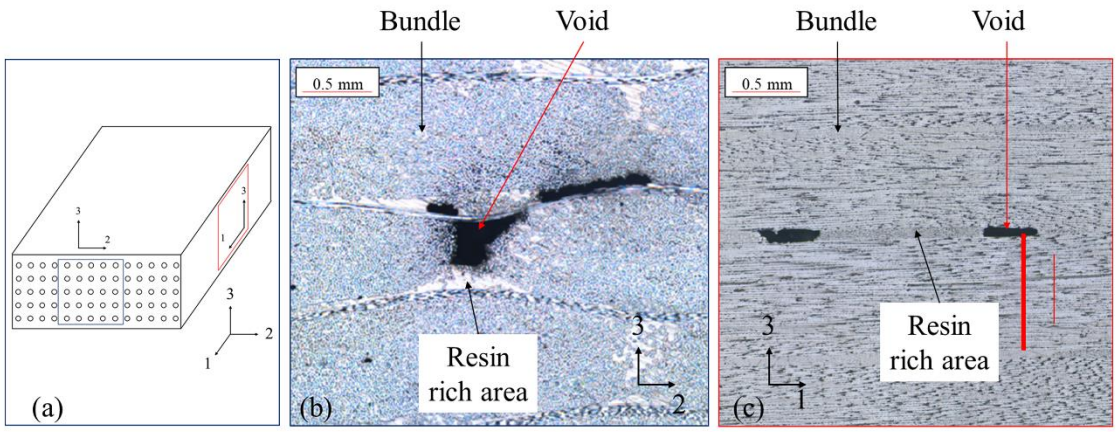

Fig. 4. (a) Laminate coordinate system; (b) intra-bundle void in the 2-3 plane; (c) intra-bundle void in the 1-3 plane

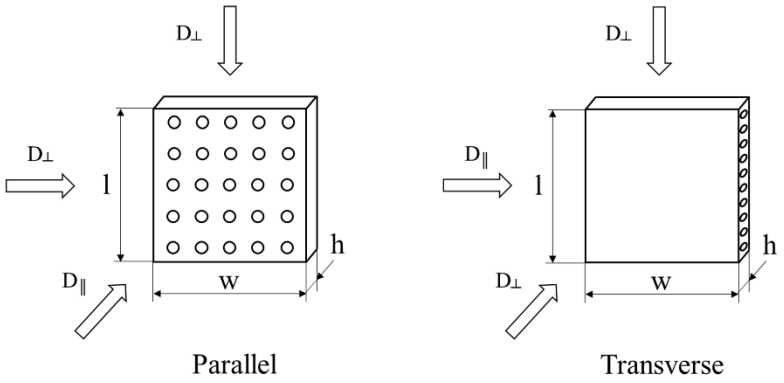

Fig. 5. Configuration of samples used for parallel and transverse diffusion measurement

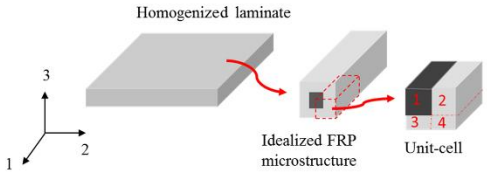

Fig. 6. A simplified microstructure of FRP composite

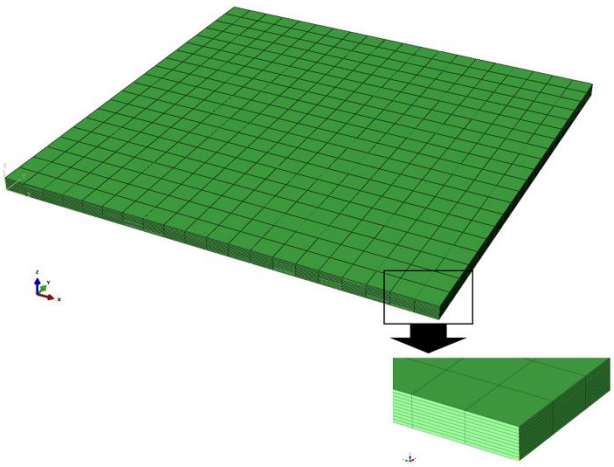

Fig.7. Mesh used for the FE analysis.

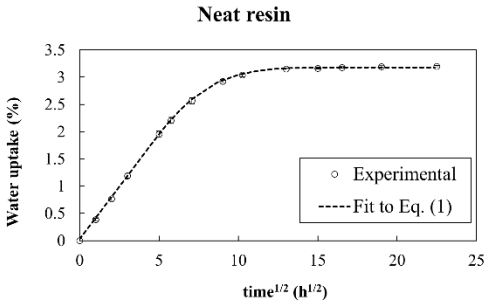

Fig. 8. Water uptake measured as % weight increase vs. time in hours. 1-D model.

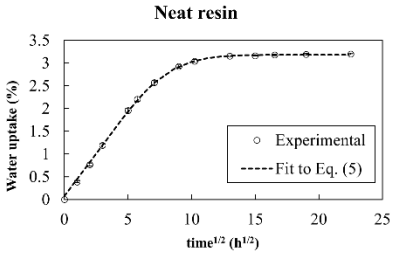

Fig. 9. Water uptake measured as % weight increase vs. time in hours. 3-D model.

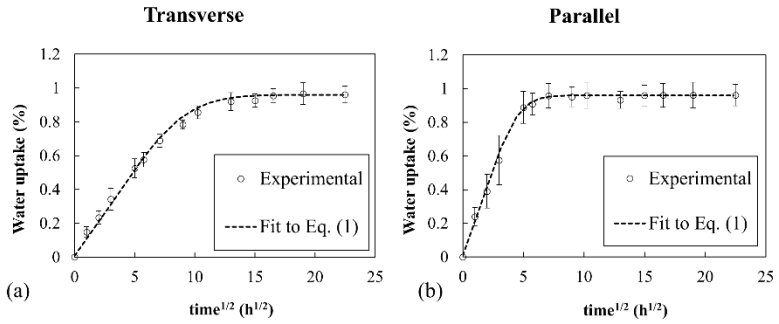

Fig. 10. Water uptake measured as % weight increase vs. time in hours, fitted with the 1-D equation.

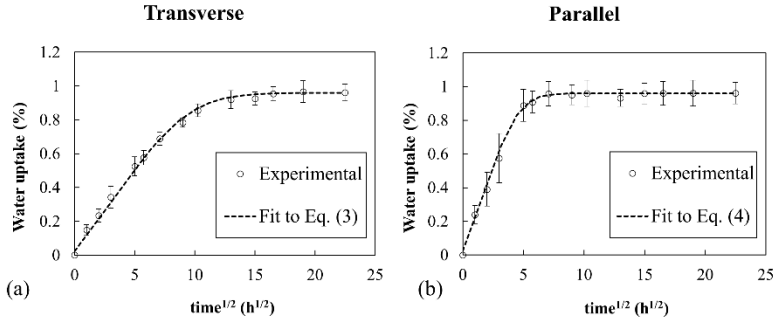

Fig. 11. Water uptake measured as % weight increase vs. time in hours, fitted with the 3-D equation.

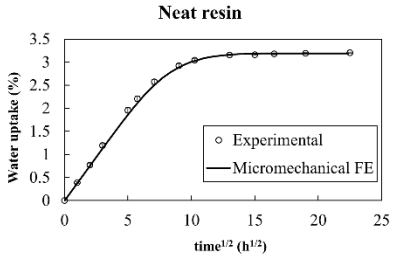

Fig. 12. Concentration of water in the resin from the micromechanics and numerical analyses.

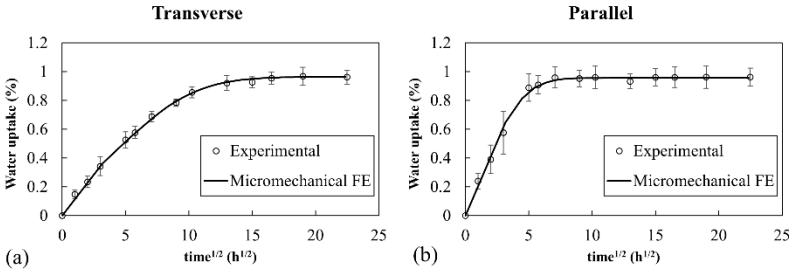

Fig. 13. Micromechanics analyses of the diffusion in FRP composites (a) transverse direction, (b) parallel direction.

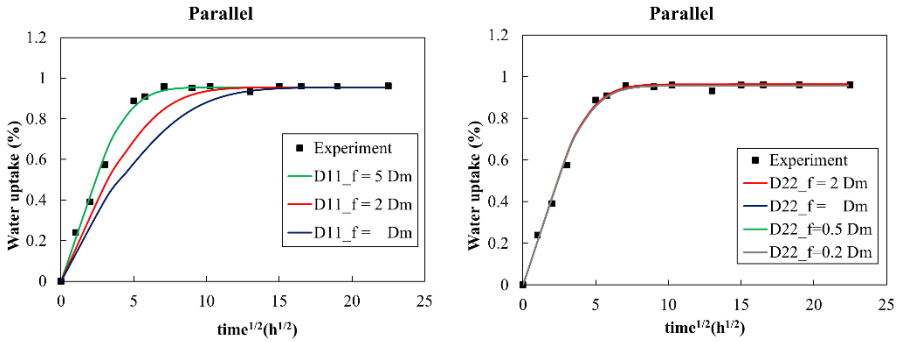

Fig. A1. Diffusion response of FRP in the parallel fiber direction: the effect of fiber anisotropy.

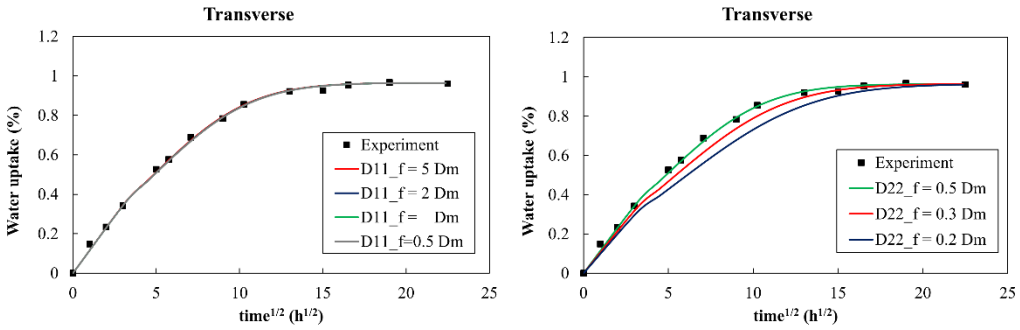

Fig. A2. Diffusion response of FRP in the transverse fiber direction: the effect of fiber anisotropy.

Tables

Table 1 Diffusivities obtained for neat resin and composite using 1-D and 3-D diffusion equation

	Neat resin	Composite	
	D (mm^2/h)	$D_\perp$ (mm^2/h)	$D_\parallel$ (mm^2/h)
1-D Equation	0.0068	0.0051	0.021
3-D Equation	0.0063	0.0045	0.020
Micromechanical FE model	0.0062	0.0042	0.020